ELSEVIER

Biochimica et Biophysica Acta 1561 (2002) 238–250

BIOCHIMICA ET BIOPHYSICA ACTA
BBA

www.bba-direct.com

Compositional domain immiscibility in whole myelin monolayers at the air–water interface and Langmuir–Blodgett films

Rafael G. Oliveira, Bruno Maggio *

Departamento de Química Biológica-CIQUIBIC, Facultad de Ciencias Químicas, Universidad Nacional de Córdoba, 5000 Córdoba, Argentina

Received 20 September 2001; received in revised form 21 December 2001; accepted 10 January 2002

Abstract

Monomolecular layers of whole myelin membrane can be formed at the air–water interface from vesicles or from solvent solution of myelin. The films appear microheterogeneous as seen by epifluorescence and Brewster angle microscopy. The pattern consists mainly of two coexisting liquid phases over the whole compression isotherm. The liquid nature of the phases is apparent from the fluorescent probe behavior, domain mobility, deformability and boundary relaxation due to the line tension of the surface domains. The monolayers were transferred to alkylated glass and fluorescently labeled against myelin components. The immunolabeling of two major proteins of myelin (myelin basic protein, proteolipid-DM20) and of 2′,3′-cyclic nucleotide 3′-phosphodiesterase shows colocalization with probes partitioning preferentially in liquid-expanded lipid domains also containing ganglioside G_{M1}. A different phase showing an enrichment in cholesterol, galactocerebroside and phosphatidylserine markers is also found. The distribution of components is qualitatively independent of the lateral surface pressure and is generally constituted by one phase enriched in charged components in an expanded state coexisting with another phase enriched in non-charged constituents of lower compressibility. The domain immiscibility provides a physical basis for the microheterogeneity found in this membrane model system.

Keywords: Monolayer; Myelin; Epifluorescence microscopy; Langmuir–Blodgett film; Lipid–protein domain; Brewster angle microscopy

1. Introduction

Complex lipid–protein monolayers at the air–water interface can be prepared from preformed lipid bilayer vesicles [1–3] and from whole natural cell membranes in aqueous solution [4,5]. The surface behavior of axolemma monolayers and the different membrane-mediated response of Schwann cells cultured onto supported Langmuir–Blodgett films of axolemma under controlled changes of membrane organization and composition was previously reported [6,7]. Recently, we described the molecular packing, surface electrostatics, surface pressure and compressibility properties of compression isotherms for monolayers prepared from whole myelin and from its total lipid fraction [8].

Epifluorescence microscopy studies have shown that coexisting immiscible liquid phases exist in films of binary lipid systems containing cholesterol and phospholipids [9–11] as well as in those formed with a complex mixture of lipids from the whole red blood cell membrane [12] and in mixtures mim-

* Corresponding author. Fax: +54-351-433-4074.
E-mail address: bmaggio@dqb.fcq.unc.edu.ar (B. Maggio).

0005-2736/02/$ – see front matter
PII: S0005-2736(02)00350-4

icking membrane lipid rafts with a liquid ordered phase state [13]. We have previously reported that monolayers from whole myelin and from its lipid fraction show a marked surface heterogeneity over the whole compression–decompression isotherm, showing phase coexistence, but the existence of compositional immiscibility was not established [14]. Calorimetric [15], wide angle X-ray diffraction [16] and spectroscopic studies [17] have indicated the existence of fluid and more ordered phases in myelin in vivo and/or in a purified fraction. Calorimetric scanning of isolated myelin shows a very broad peak of heat capacity [15], beside two sharp peaks ascribed to irreversible denaturation of proteins. Monolayer phase transitions can be observed in simple systems with few (one–three) components [18,19]. In the case of whole myelin and the total myelin lipid fraction, with probably more than 100 different lipid and protein species, approximately isobaric, classical surface pressure-induced two-dimensional phase transitions become undetectable in compression isotherms [8]. The lack of this type of transitions in multicomponent films should be expected since the cooperativity of phase transitions decreases dramatically as the complexity and number of interactions increase in the system [20]. Similarly, phase coexistence due to non-mixing behavior in monolayers might be detected in principle by the presence of multiple collapse points if the collapse pressure of each phase is different from that of the other [21], but whole myelin shows a single and sharp collapse point. Immiscibility of phases with different compositions could account for the micro-heterogeneity observed with epifluorescence microscopy. This technique allows exploration of the surface topography and component distribution in the different phases due to non-mixing behavior, by direct observation of laterally separated phase domains. These are revealed by fluorescent lipid probes that can differentiate liquid-expanded and more ordered or condensed phases [22]. In order to test immiscibility, individual myelin components were labeled after monolayer transfer to Langmuir–Blodgett films. This 'fixes' the monolayer in the conditions of transfer to the solid support rendering a stable interface capable of resisting manipulation during the labeling procedure (a binding assay with a fluorescent ligand or a simplified fluorescence immunochemical assay in which the chemical fixation step is avoided).

The probes used also give information about the physical state of the phase in which they are partitioned. Apart from uncertainties arising from some phase squeezing out of fluorescent lipid probe or residual probe miscibility dependent on pressure [22], the lipid probes used herein prefer liquid-expanded phases, and are not favorably partitioned in phases of higher order or packing such as the liquid condensed and cholesterol-enriched phases. On the other hand, Brewster angle microscopy (BAM) is a non-perturbing technique also allowing direct observation of monolayer films. By using a p-polarized laser beam incident on a clean water surface at the Brewster angle a minimum reflection is achieved. The presence of a monolayer at the interface causes an increment of the reflection due to changes of molecular density, surface thickness or refractive index [23,24]. In this work we have investigated the domain heterogeneity of myelin monolayers at the air–water interface as a function of the lateral surface pressure, by complementary observation of the film by both epifluorescence and BAM. Also, using Langmuir–Blodgett films we have ascertained compositional domain heterogeneity by specific labeling of representative lipid and protein components of myelin in the different coexisting surface phases.

2. Materials and methods

2.1. Materials

The probes *N*-(7-nitrobenz-2-oxa-1,3-diazol-4-yl)-diacyl phosphatidylethanolamine (NBD-PE) [25,26] and *N*-(lissamine rhodamine B sulfonyl)diacyl phosphatidylethanolamine (RHO-PE) were from Avanti Polar Lipids (Alabaster, AL, USA). Both are head group labeled, with 55% acyl chain unsaturation, made from egg phosphatidylcholine, which favors their partition in liquid-expanded phases. Serum anti-myelin basic protein (anti-MBP) was obtained from rabbit with experimental allergic encephalomyelitis, previously injected with myelin basic protein (MBP) in Freund's coadjuvant. Monoclonal antibody anti-2′,3′-cyclic nucleotide 3′-phosphodiesterase (anti-CNPase), anti-galactocerebroside (anti-

GalCer), fluorescein isothiocyanate-labeled B subunit of cholera toxin (FITC B cholera toxin), the cholesterol binding antibiotic Filipin III from *Streptomyces filipinensis* [27,28] and anti-rabbit IgG (whole molecule FITC conjugate) were from Sigma (St. Louis, MO, USA); anti-proteolipid-DM20 (anti-PLP) directed against CGRGTKF (C-terminal region) was from Serotec (Oxford, UK). The phosphatidylserine binding protein Annexin V Alexa Fluor [29] was from Molecular Probes (Eugene, OR, USA). Anti-mouse IgG tetramethyl rhodamine isothiocyanate labeled was from Jackson ImmunoResearch Laboratories (West Grove, PA, USA).

2.2. Myelin and lipids

Highly purified myelin was prepared from bovine spinal cord [30]. Myelin was vesiculated in phosphate buffer 1 mM pH 8, 2 mM dithiothreitol [31]. The vesicles were resuspended in the same buffer to a final protein concentration of 0.24 mg/ml, and passed five times through a 26 G needle fitted to a syringe. Also, myelin vesicles were dissolved in 19 vols. of chloroform–methanol (2:1) [32] and immediately used for monolayer spreading [8].

Total lipids from myelin were extracted with 19 vols. of chloroform–methanol and partitioned with 4 vols. of water overnight [33]. The resulting lower phase after Folch's partition was dried under nitrogen and redissolved in chloroform–methanol (2:1); this process was repeated twice. Phospholipid phosphorus was measured by the modified microprocedure of Bartlett [34]. Total proteins were determined by the method of Lowry [35] in the presence of 0.2% sodium dodecyl sulfate using bovine serum albumin as standard.

2.3. Epifluorescence and BAM of monolayers

Monolayers were obtained as previously described [8] by spreading a suspension (0.24 protein mg/ml) of myelin vesicles or by spreading a freshly prepared solution of myelin dissolved in 19 vols. of chloroform–methanol (2:1). The latter procedure allows direct incorporation of fluorescent lipid probes in the solvent solution. As previously reported, the isotherm of the myelin monolayer prepared in either manner is indistinguishable [8]. Similar equivalence in the behavior of lipid–protein monolayers formed from solvent solutions and from vesicles has been previously reported, including the surface domain pattern formed for more simple systems [3]. The solutions were doped with 2 mol% of NBD-PE [25,26] or 0.25–0.5 mol% of RHO-PE. The subphase was 10 mM tris(hydroxymethyl aminomethane) buffer in 100 mM NaCl, 20 mM $CaCl_2$, adjusted to pH 7.4 with HCl. With few exceptions, the surface pressure reached in the initial spreading was below 0.3 mN/m. The overall lipid and protein composition of monolayers prepared from whole myelin is very similar to that of the whole myelin fraction [8]. The lipid and protein components of myelin distribute asymmetrically along the transverse plane of the natural membrane [36] and this essentially means that the components of the two bilayer halves of the natural myelin membrane are mixed in the myelin monolayer. No attempt is made to ascribe conclusions on the surface topography of myelin monolayers to that of the natural myelin membrane. After monolayer spreading the films were compressed at a rate of 0.3 nm^2/molecule/min; 5–15 min of equilibration were allowed after each change of surface pressure before image capturing (this is reflected as small drops in surface pressure in Fig. 1A). Although the equilibration time is in the operational period frequently employed and affords reproducibility, it should be emphasized that the surface patterns observed by surface microscopy in this type of studies correspond to relatively long-lived, but metastable, molecular distributions that are usually not in true thermodynamic equilibrium; similar to more simple lipid systems, equilibration times of the order of days or weeks may be required [37]. The observations were carried out after discontinuous isometric compression of the monolayers at room temperature using a KSV Minitrough II (KSV, Helsinki, Finland) mounted on the microscope stage. An open-end Teflon mask with a lateral vertical slit, extending through the film into the subphase, was used in order to restrict lateral monolayer flow in the field being observed. A Zeiss Axioplan, or an Axiovert (Carl Zeiss, Oberkochem, Germany) epifluorescence microscope was used, equipped with a mercury lamp HBO 50, and objectives of 10 and 20×. Exposure times were typically between 0.1 and 1 s. The pictures were registered by a CCD video camera (Micromax,

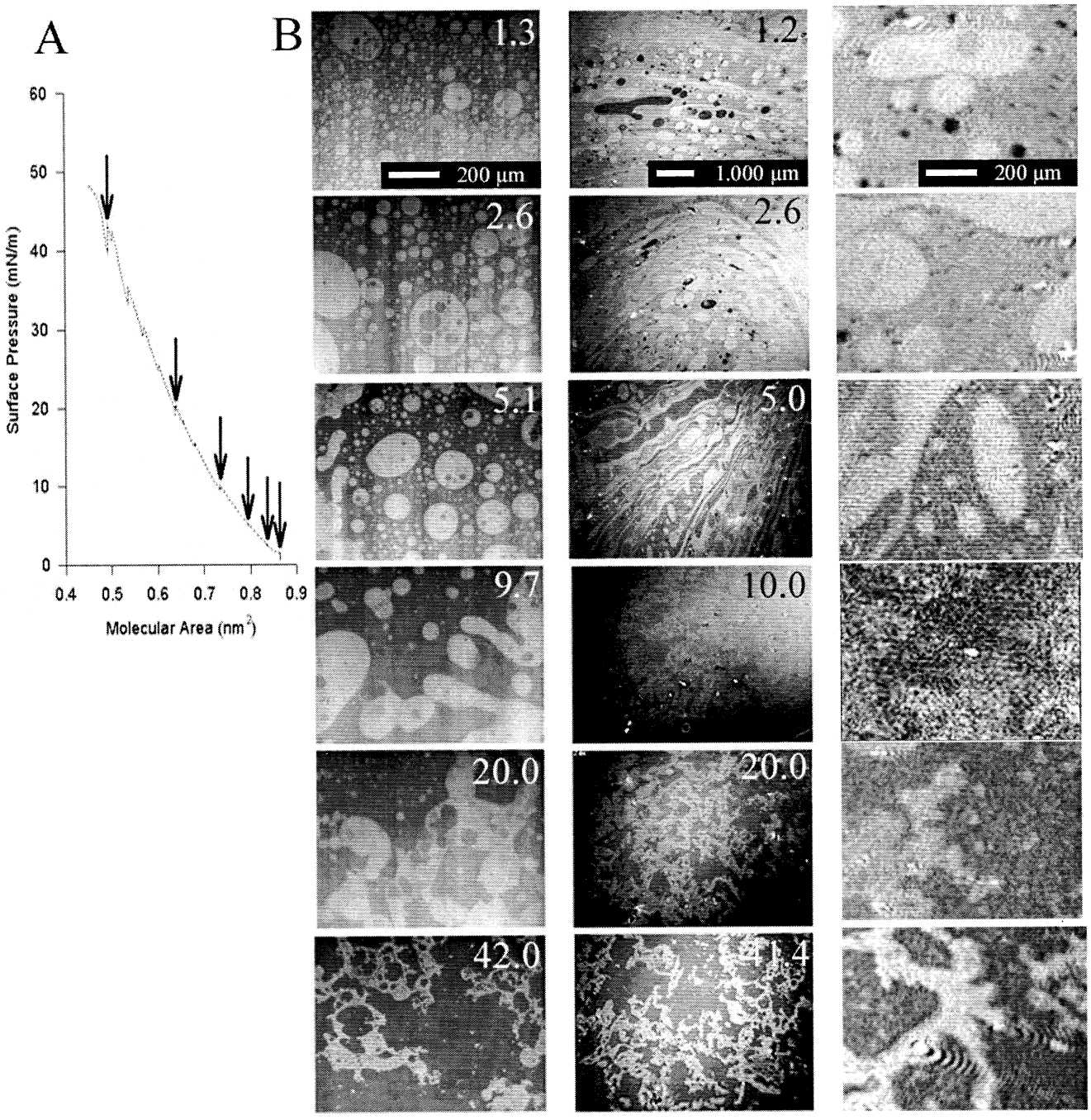

Fig. 1. The surface pressure–molecular area isotherm by discontinuous compression of the whole myelin monolayer is shown in A. The arrows indicate the points of image capturing of the patterns shown in B. The left column in B corresponds to epifluorescence microscopy (using 0.5 mol% of RHO-PE). The middle column in B corresponds to BAM. The figures in both columns indicate the surface pressure in mN/m. The right column is a magnification of the BAM images shown in the middle column.

Princeton Instruments, USA) commanded through Metamorph 3.0 software (Universal Imaging Corporation, PA, USA). For BAM essentially the same procedure as in epifluorescence microscopy was followed. A MiniBam microscope from Nanofilm Technologies was used (NFT, Göttingen, Germany) and images were recorded with the software provided by the manufacturer.

2.4. Myelin Langmuir–Blodgett films

The myelin monolayer was coated onto alkylated glass coverslips as described previously [6,38]. Briefly, coverslips (12 mm diameter) were first alkylated with octadecyltrichlorosilane in order to self-assemble a covalently linked monolayer of octadecylsilane. The quality of the hydrophobic coverage of each coverslip was checked before use on the basis of the contact angle and free-running of double-distilled water droplets deposited on their surface. The alkylated coverslips, held horizontally above the monolayer set at the desired constant surface pressure, were lowered until they gently touched the monolayer surface. The coverslip was left to rest over the surface for 15 s at constant surface pressure, and then pushed vertically through the monolayer at a speed that was synchronized with the servo-surface pressure barostat in order to automatically keep the surface pressure constant during coating. When the monolayer is successfully transferred to the alkylated coverslip a simultaneous decrease of the monolayer area occurs that was automatically recorded in each case. The Langmuir–Blodgett films thus obtained were always handled under aqueous solutions to avoid the collapse of the monolayers. These films were labeled by incubating from 1 to 12 h with specific ligands at room temperature. 10–63× objectives were used with the same equipment as described above, or a photographic camera using 400–1600 ASA film. Filter sets were the standard for epifluorescence microscopy, except for that used for Filipin III, consisting of a wide band exciter (330WB80) for UV irradiation, and a long pass emitter (400ALP), both from Omega Optical (Brattleboro, VT, USA), and a 380 nm beamsplitter (380DCLP) from Chroma Technology (Brattleboro, VT, USA).

3. Results

3.1. Surface domains during compression

We have checked that NBD-PE does not modify the compression behavior of the total myelin lipid fraction or of the whole myelin monolayers. RHO-PE gives the same pattern as that observed with NBD-PE as expected because both probes partition preferentially in liquid-expanded phases (both probes are synthesized from transphosphatidated egg lecithin and contain identical aliphatic chains). Fig. 1A shows the compression isotherm. The monolayer domain patterns at defined surface pressure are shown in Fig. 1B. The small drops in surface pressure over the curve are due to the visco-elastic relaxation of the film (which occurs in the range of several minutes during image capture) and not to overcompression above the equilibrium spreading pressure. The equilibrium spreading pressure of the whole myelin monolayer is around 47.5 mN/m, the same as the collapse pressure [8].

Representative patterns of surface domains of the myelin monolayers during compression, revealed by lipid probe partitioning, are shown in Fig. 1B as observed by epifluorescence (10× objective; left column) and by BAM (middle column). In order to compare the images it should be realized that the linear magnification in BAM is 7 times lower and that the contrast is frequently lower. In order to facilitate comparisons we have amplified fields of the middle column BAM images (right column); their total magnification is that of the left column, although the resolution is lower (about 20 μm). Taking into account the different scales, the domains revealed by both techniques at the different surface pressures correspond to the same surface pattern. This consists mainly of two phases which are evidenced by both epifluorescence and BAM (Fig. 1B). The bright and dark phases correspond to the same kind of domains with both techniques, at least

→

Fig. 2. The micrographs show the double labeling of myelin components and NBD-PE (liquid-expanded phase). (a,b) Anti-MBP and NBD-PE 12 mN/m; (c,d) anti-MBP and NBD-PE 33 mN/m; (e,f) anti-MBP and FITC B cholera toxin 12 mN/m; (g,h) anti-MBP and FITC B cholera toxin 42 mN/m; (i,j) anti-CNPase and NBD-PE 12 mN/m; (k,l) anti-CNPase and NBD-PE 42 mN/m; (m,n) anti-PLP and NBD-PE 12 mN/m; (o,p) anti-PLP and NBD-PE 42 mN/m; (q,r) preimmune antiserum and NBD-PE 33 mN/m; (s,t) anti-MBP (lipid monolayer) and NBD-PE 33 mN/m.

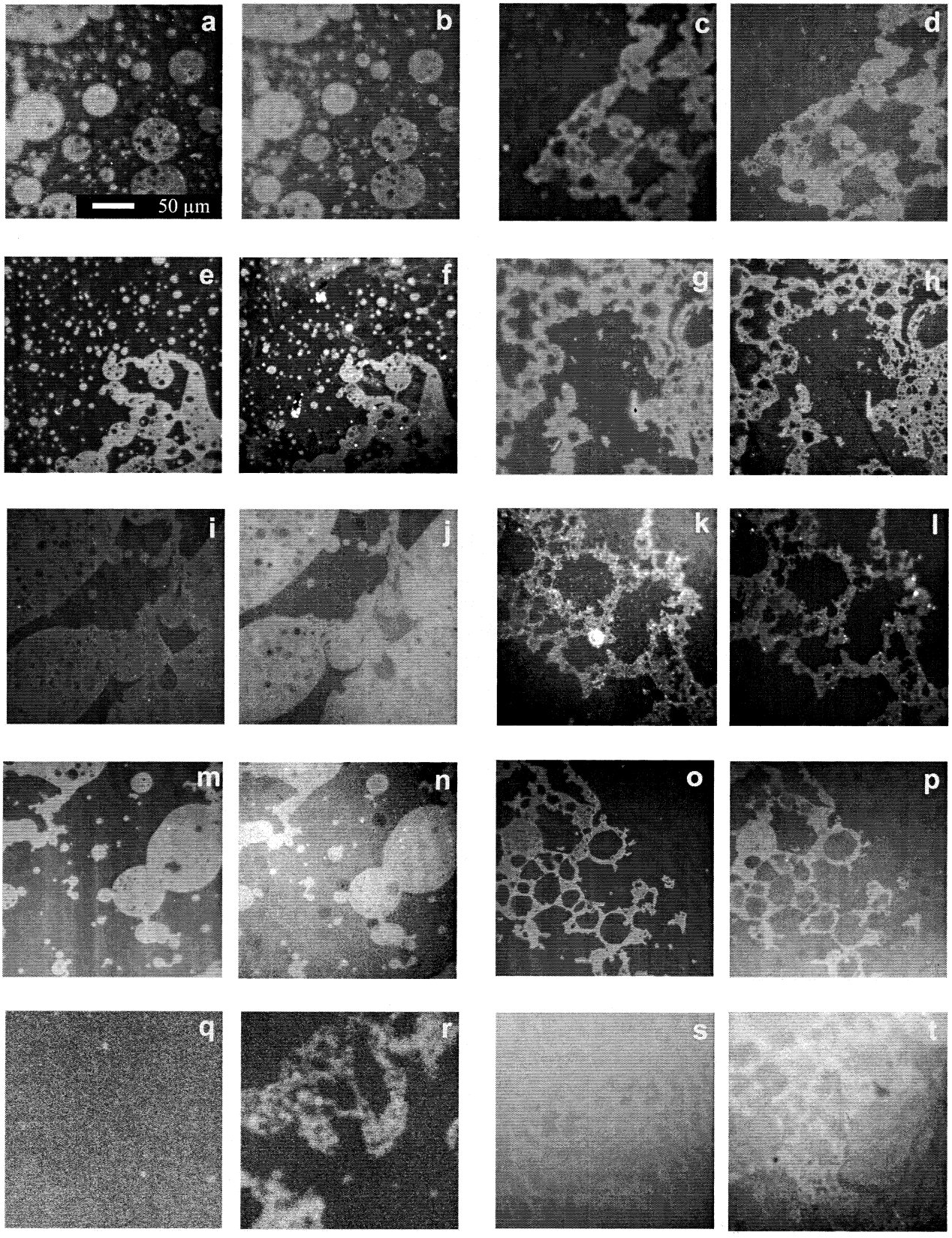
a
50 μm
b
c
d
e
f
g
h
i
j
k
l
m
n
o
p
q
r
s
t

in the images at high surface pressure. With BAM, at about 10–15 mN/m the contrast is lowered, and the film appears optically homogeneous in a range of 2–4 mN/m; nevertheless the epifluorescence images show the existence of microheterogeneity. It should be considered that in images of a pure phospholipid the contrast is inverted in BAM with respect to that revealed by the liquid-expanded probes [39]. This occurs in BAM because the increased optical thickness of the more ordered phase leads to reflection of more light, while fluorescent probe partitioning is insensitive to thickness. Nevertheless, with our current equipment, the optical thickness cannot be quantitatively ascertained and could be altered by compositional heterogeneity (see below). Topographically, the bright phase at low surface pressure is mainly sequestered into circular clusters within the deep dark phase, although some dark clusters may be found distributed inside bright clusters, giving a nested structure. The relaxation of the boundaries due to line tension indicates the fluid nature of the two phases, at least below 20 mN/m. In some fields, the circular domains of the bright phase form a pattern with a spacing regularity between the domains (Fig. 1B left column, 1–5 mN/m) of the order 10 μm. Some long-range organizing effect appears to dominate the distribution of these bright small circular domains that are dispersed as separated as possible within the dark phase. These small circular domains exhibit Brownian motion and are included within an apparently fluid phase from which the probe is excluded; occasionally they can undergo lateral fusion

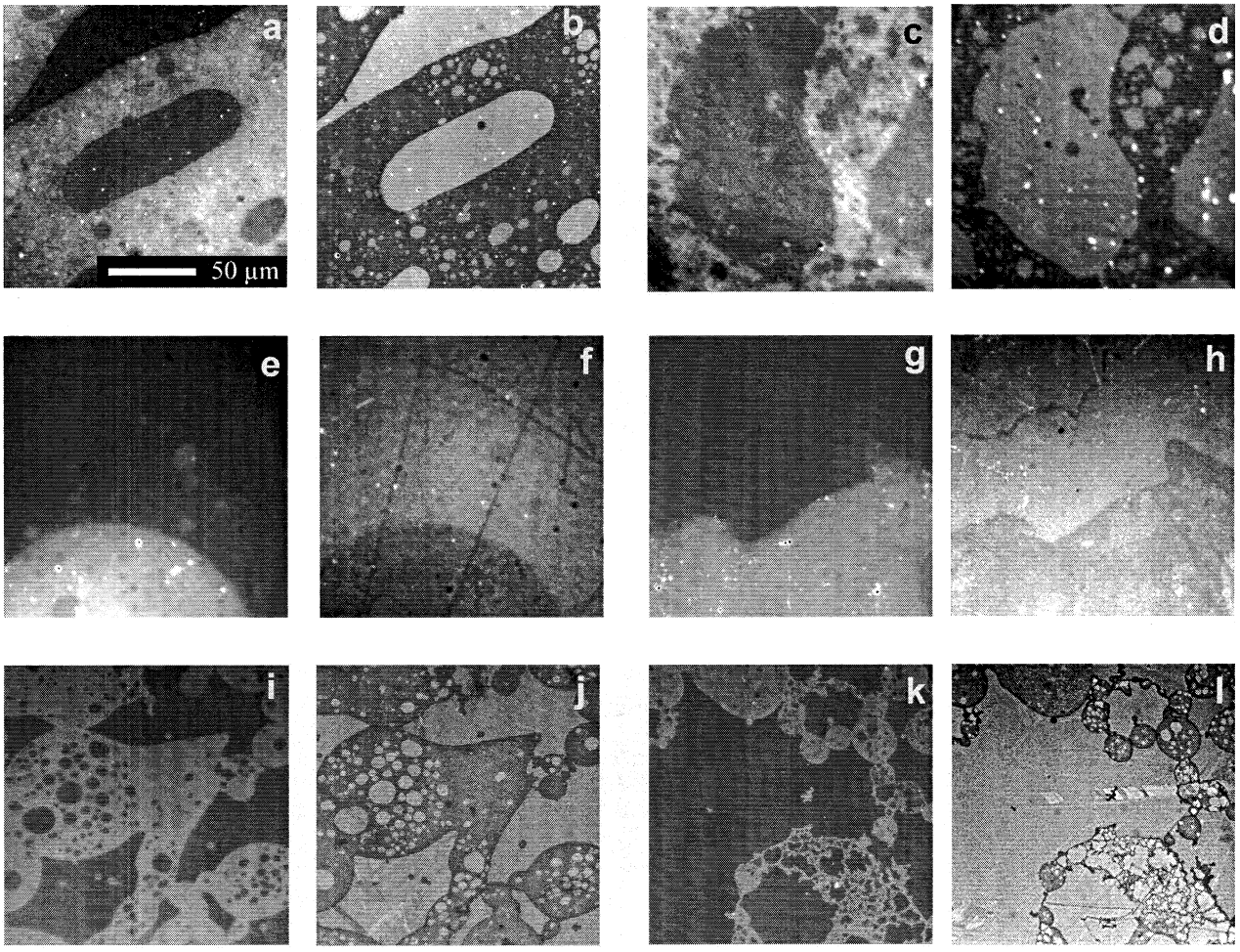

Fig. 3. The micrographs show the double labeling of myelin components showing inverse localization with respect to the liquid expanded phase probes. (a,b) Anti-Galcer and RHO-PE 12 mN/m; (c,d) anti-Galcer and RHO-PE 42 mN/m; (e,f) Filipin and NBD-PE 12 mN/m; (g,h) Filipin and NBD-PE 42 mN/m; (i,j) Annexin V and anti-PLP 12 mN/m; (k,l) Annexin V and anti-PLP 42 mN/m.

after contact. Beyond a diameter of approx. 200 μm, the bright clusters become increasingly distorted to more elliptical shapes; these large clusters (as long as several millimeters) are easily seen in BAM images, but small clusters and their ordered spacing are beyond the resolution of our BAM. Also, we have occasionally observed a gray phase at low surface pressure, having highly irregular boundaries and poor reproducibility [14]. A crisp fractal-like structure is increasingly formed as the surface pressure grows from 20 mN/m to the collapse point (Fig. 1B, 20 and 42 mN/m). These images show a self-similarity that extends over the range scale observed. Note that in the BAM images the vertical side is 4.8 mm and in fluorescence images 0.7 mm; nevertheless the pattern remains very similar. At 10–20 mN/m an intermediate pattern is observed between the circular and the fractal domains, the latter being apparently formed by the merging and distortion of the polydispersed circular and elliptical domains.

3.2. Compositional domains in Langmuir–Blodgett films

After the transfer of the film, the pattern revealed by the fluorescent lipid probes is similar to that observed in monolayers at the air–water interface. This is not altered by subsequent labeling with the other markers employed (fluorescent antibodies and other specific ligands). The coated monolayers are mechanically stable, showing high resistance to handling, stress, or dragging forces. The patterns are stable for at least 3 or 4 days at room temperature and the immunolabeling renders the film more stable and capable of supporting air exposure without collapse (different from transferred films that were not immunolabeled). Fig. 2 shows that immunolabeling of MBP colocalizes with NBD-PE either at 12 (Fig. 2a,b) or 33 mN/m (Fig. 2c,d). Control experiments (Fig. 2q,s) did not show labeling when the monolayer of whole myelin was incubated with rabbit preimmune antiserum (Fig. 2q), or when the monolayer consisted of the extracted total myelin lipid fraction free of MBP (Fig. 2s). Fig. 2e–h shows that ganglioside G_{M1} labeling (revealed by FITC B cholera toxin) colocalizes with anti-MBP and thus within the more liquid-expanded phases, both at 12 and 42 mN/m. Fig. 2i–l shows that the labeling for CNPase also colocalizes in the domains labeled by NBD-PE at 12 and 42 mN/m. Fig. 2m–p shows the colocalization of anti-PLP-DM20 with NBD-PE, either at 12 and 42 mN/m. It can be seen in Fig. 2 that the patterns shown in Fig. 1B are conserved after film deposition on the solid support; the same occurs with the patterns shown in Fig. 3. This figure shows distribution of component markers that are not located in the liquid-expanded phase. The labeling with anti-GalCer shows a 'complementary' pattern to that of NBD-PE (Fig. 3a–d) at 12 and 42 mN/m. Both the cholesterol binding antibiotic Filipin III [27,28] (Fig. 3e–h) and the phosphatidylserine binding protein Annexin V [29] (Fig. 3i–l) also show the same inverse pattern and localization. The contrast shown in the case of Annexin V was done with anti-PLP-DM20; the same results are obtained with RHO-PE. Table 1 summarizes the localization of markers in the different phases.

Table 1
Preferential localization of different myelin component labeling on its Langmuir–Blodgett film phases

Component	Localization in phase type
RHO-PE	Liquid expanded
NBD-PE	Liquid expanded
MBP	Liquid expanded
PLP	Liquid expanded
CNPase	Liquid expanded
Ganglioside G_{M1}	Liquid expanded
Cholesterol	Cholesterol enriched
Galactocerebroside	Cholesterol enriched
Phosphatidylserine	Cholesterol enriched

4. Discussion

4.1. Surface domains during compression

The results indicate that the coexistence of domains of different phases, as revealed by the differential surface partitioning of NBD-PE at 2 mol% and by RHO-PE at 0.25–0.5 mol%, is a fundamental feature of whole myelin monolayers at the air–water interface. This is supported by BAM (which does not require addition of probe). In BAM, the liquid-expanded phase appears brighter, in keeping with the fact that this is a protein-enriched phase which is

probably thicker (see below), similar to what has been observed for streptavidin binding on biotinylated lipid monolayers [40]. The microscopic techniques indicate that microheterogeneous surface phases of different composition coexist in myelin monolayers over the whole surface pressure–molecular area isotherm. NBD-PE, and similar unsaturated acyl chain probes, partition preferentially in liquid-expanded phases. These probes are excluded from liquid-condensed (as shown in DPPC two-dimensional phase transition [26]) and from cholesterol-enriched phases, probably analogous to the bilayer liquid-ordered phases (as those formed in mixtures with a cholesterol molar fraction higher than 0.2–0.4 [9–13]). The cholesterol-enriched phase in monolayers is increasingly related to the liquid-ordered phase adopted in bilayers [41] and/or detergent insoluble fractions (lipid rafts) of membranes [11,13,42].

The topographical behavior may be summarized as consisting of two well defined structures: mostly rounded (below 100 μm radii) and large elongated clusters of liquid-expanded and cholesterol-enriched phases (see below) up to 20 mN/m, and a progressively established fractal-like pattern above 20 mN/m. The general superstructure appears to be due to long range repulsive interactions (as revealed by the regular spacing among the small bright circular cluster) and by line tension effects (the one-dimensional lateral analogue of surface tension) as revealed by the roundness of the fluid–fluid boundaries, relaxing in this manner the interfacial (linear) excess Gibbs free energy. It should be noted that, as reported in a previous work [14], not all the lateral interfaces are rounded as might be expected for liquid–liquid interfaces. Occasionally a third phase that is not liquid may be observed up to 20 mN/m [14], but the reproducibility of the occurrence of this solid phase is low. At 1–5 mN/m, the line tension and dipolar repulsion appear to dominate the general pattern, giving a structure very similar to that described for mixtures of saturated phospholipids and cholesterol at a molar fraction of 0.3–0.4 [10,11,43]. The line tension rounds the lateral interfaces and the repulsion gives a regular spacing between liquid-expanded domains [43]. The spacing between the liquid-expanded clusters is in the order of 10 μm, which is beyond the resolution limit of our BAM instrument. Beyond domain radii of about 100 μm, the circular clusters become increasingly unstable and acquire more elliptical shapes; further increments of size lead to very elongated domains (sometimes distorted) as seen in the broader field resolved by BAM. According to McConnell [43] the equilibrium domain radius is smaller by a factor $e^{-1/3}$ (which would lead to radii of about 70 μm). Also, the domains with radii smaller than 35 μm represent non-equilibrium sizes. On compression, the long range order is progressively lost, as seen by the decay in the regularity of the pattern beyond 5 mN/m. Also the line tension effect is weakened as seen by the decay of the roundness of the boundaries. We ignore at present if this is due to a real drop in the electrostatic and interfacial forces, or if this is an effect of increased viscosity of the film. Drops of the line tension have been estimated for cholesterol–dimyristoylphosphatidylcholine mixtures [44] being an inverse linear function of surface pressure up to the mixing point. Also, in myelin lipids we have shown a mixing behavior at about 20 mN/m, which implicates a zero line tension in the protein free system. Presently we do not know the protein effect on the domain boundary stability.

We previously described intermolecular reorganization of the monolayer from whole myelin based on the existence of defined discontinuities in the surface pressure–molecular area and surface potential/molecule area isotherms occurring at about 20 mN/m that was ascribed to the presence of protein [8]. We have also noted that myelin lipid monolayers show a small but reproducible drop in the electrostatic surface potential/molecule at a surface pressure between 17 and 22 mN/m. The topographical pattern displayed by the whole myelin monolayer below 20 mN/m is very similar to that found for the monolayer of the total myelin lipid fraction, but at 20 mN/m a homogeneous phase is observed in the latter [14]. As for other systems reported in the literature [43], it is likely that the superstructure below 20 mN/m is maintained by electrostatic or dipolar repulsion (which prevents boundary relaxation to take place), leading to mostly ordered patterns distorted by the polydispersity of the clusters. In the compression process the mechanical work done on the lipid film allows surface homogenization and, on the other hand, a drop of the surface potential per molecule occurs, indicating an average reorientation of dipoles. Near 20 mN/m, an overall reorganization

takes place, and the components in the film appear to homogeneously mix into a rather amorphous liquid state. In whole myelin monolayers the mechanical work of compression at about 20 mN/m is enough to overcome the repulsion between the bright liquid-expanded domains. The latter should be the phase including the greater dipole density [43], which is in keeping with its regular spacing, thickness and the presence of protein compared to the other, cholesterol-enriched, phase (see below). The surface domain revealed by epifluorescence microscopy of lipid monolayers mimicking the inner and outer leaflet of the erythrocyte membrane showed a pattern, at pressures below 20 mN/m, that is very similar to that found in our work with myelin monolayers. Also, it was described that the reconstituted erythrocyte lipid mixtures show critical mixing behavior at a surface pressure point of 21 and 29 mN/m [12].

The similarity of our patterns with those reported for the mixture reconstituted from erythrocyte lipids could arise from the presence of liquid-expanded and cholesterol-enriched phases, the latter excluding the fluorescent lipid probes [12]. This behavior is promoted by a high mol fraction of cholesterol (0.5 in the erythrocyte membrane). Cholesterol is a major determinant for the existence of liquid-ordered phases in bilayers. By X-ray diffraction this lipid is found in both monolayer halves of the myelin membrane, with the mol fraction of cholesterol in the outer monolayer nearly twice that found in the inner monolayer [36]. We have determined by monolayer collection and subsequent analysis a cholesterol mol fraction of 0.42 in the myelin monolayer [8], almost equal to that found in myelin. So, although the compositional difference of the two halves is lost in the monolayer, both halves share the more abundant lipid (cholesterol), and this component is probably a major determinant for the phase coexistence described.

The miscibility properties of the probes selectively detect that the monolayer surface is not homogeneous at all surface pressures, in agreement with immunofluorescence and BAM. The domains are very mobile and deformable by lateral stress and surface flow: at high surface pressures the film becomes progressively more viscous. Up to 10 mN/m the fluid circular and elliptical bright clusters are mostly included in the dark phase. It is unlikely that the latter correspond to a condensed rigid phase (which would be consistent with the lack of fluorescent probe within it) because of the round shape of its boundary indicating a relaxation process due to line tension. Moreover, small point-like brilliant fluid clusters can be visually seen to undergo lateral Brownian motion, indicating that the dark surrounding matrix is a liquid, in spite of the probe being immiscible in this phase. Moreover, rotation of the analyzer from the plane of polarization under BAM visualization does not reveal features suggesting changes in molecular tilting in either phase, compatible with their liquid nature [39].

4.2. Compositional domains in Langmuir–Blodgett films

We followed the labeling of individual components by epifluorescence of Langmuir–Blodgett films, using specific fluorescent ligands. The quantities in the text given below indicate the mol fraction of lipids or weight percentage of protein previously quantified in monolayers collected from the air–water interface [8].

Double labeling experiments indicate that there are two compositional phases, one that contains the probes for the liquid-expanded phase (NBD-PE and RHO-PE), ganglioside G_{M1} (0.5%), and myelin proteins, namely CNPase (10% of total myelin protein mass) MBP (35%), PLP and DM20 (50%). These protein components account for over 85% in weight of the total protein mass. The second phase is enriched in cholesterol (42%), galactocerebroside (15%) and the anionic phospholipid phosphatidylserine (7%); these lipids account for 64 mol% of the total lipids of myelin. The rest of the lipid components in myelin monolayers are phosphatidylcholine (7%), phosphatidylethanolamine (15%), sulfatide (3%) and sphingomyelin (9%) [8]. These figures are very similar to those given for purified myelin [45].

The distribution pattern is independent of the surface pressure of the film, indicating that the surface topography of myelin monolayers shows microheterogeneous phase coexistence mainly derived from compositional immiscibility of surface domains. In summary, it appears that in the myelin film there are at least two phases of very different composition: on one side the liquid-expanded phase in which the labeled components are liquid expanded and contain

a charged hydrophilic group (ganglioside G_{M1}) [18] or basic proteins (the isoelectric point for PLP is >9 [46], for CNPase about 8.6–9 [47] and for MBP >10 [48]), and another phase containing predominantly uncharged and condensed components such as galactocerebroside, cholesterol and also including the anionic phosphatidylserine.

The preferential distribution of non-GPI-anchored proteins in the liquid-expanded phases is in keeping with available evidence regarding their location in more easily deformable liquid-expanded phases [49,50]. This facilitates protein insertion, may accommodate hydrophobic length mismatch, and reduce interfacial tension caused by lateral defects that are not easily supported by more ordered phases [51], as those promoted by cholesterol. In whole myelin monolayers the presence of myelin proteins abolishes the mixing point found in the total lipid fraction monolayer at about 20 mN/m [14], and appears to establish a 'surface frame' into which the lipids are constrained to distribute. This is in agreement with reports indicating coexistence of different phases in the myelin surface in which the general thermotropic properties appear derived from the behavior of the lipid fraction while a phase ordering role may be assigned to the protein fraction of myelin [16]. On the other hand, the surface of natural myelin is also conceived as organized in phase-separated lipid–protein microdomains whose structure depends on composition and molecular organization [52].

Interestingly, certain procedures and chemicals (tetracaine, calcium, glycerol, dimethyl sulfoxide, dehydration and hypertonic solutions) generate two lateral phases of nerve myelin [36]. Moreover, freeze etching has detected phase domains depleted of intramembranous particles (proteins) and with a decreased period (spacing of 120–130 Å) or thickness (compacted myelin). The 12–15 Å of aqueous space do not permit the presence of proteins that are the natural spacers of the apposed bilayers. The myelin structure with normal period is very enriched in intramembrane particles and thicker. The phase domains are present in register in both halves of the membrane, as seen in cross-section, and typically prolong for up to 100 monolayers.

The idea of liquid-ordered phases existing in myelin (probably equivalent to our cholesterol-enriched phase in myelin monolayers) is currently being suggested [53]. Studies of detergent solubilization indicate a compositional heterogeneity in myelin. It was shown that myelin contains detergent insoluble fractions ('lipid rafts'), containing cholesterol, galactocerebroside and galactosulfocerebroside, similar to our present work. These detergent insoluble lipid rafts are also enriched in PLP [54]. Regarding the latter, our results are different since PLP labeling does not colocalize with the labeling of cholesterol and galactocerebroside. It should be emphasized that the surface topography described in this work does not necessarily correspond to the real phases present in the natural myelin surface, because, as stated initially, the components of both membrane halves have been combined in one monolayer and bilayer spanning membrane proteins (such as PLP) may suffer denaturation and/or relocation in the monolayer. Also, during the detergent extraction utilized for isolating lipid rafts, the system may suffer rearrangement. Comparisons between the two systems are difficult.

In conclusion, it appears possible that in myelin bilayers [53] and monolayers the lipid raft composition is unusual, due to the high galactocerebroside content compared with any other membrane. Our results indicate that cholesterol and galactocerebroside colocalize in the same lipid domain.

Our observations provide new insights into the basic features of dynamical microheterogeneous patterns displayed in a complex interface formed by a natural mixture of myelin components under known intermolecular organization and the techniques implemented provide means of exploring further questions related to the structural dynamics of these natural membrane surfaces keeping well controlled molecular conditions.

Acknowledgements

This work was supported in part by SECyT-UNC, CONICOR, FONCYT y CONICET, Argentina. R.G.O. is a fellow and B.M. is a principal career investigator from CONICET. We thank Dr. Alicia Degano and Dr. German Roth for the generous gift of anti-PLP and anti-MBP antibodies.

References

[1] H. Schindler, Exchange and interactions between lipid layers at the surface of a liposome solution, Biochim. Biophys. Acta 555 (1979) 316–336.

[2] Th. Schürholz, H. Schindler, Lipid–protein surface films generated from membrane vesicles: self-assembly, composition, and film structure, Eur. Biophys. J. 20 (1991) 71–78.

[3] K. Nag, J. Perez-Gil, A. Cruz, N.H. Rich, K.M.W. Keough, Spontaneous formation of interfacial lipid–protein monolayers during adsorption from vesicles, Biophys. J. 71 (1996) 1356–1363.

[4] R. Verger, F. Pattus, Spreading of membranes at the air–water interface, Chem. Phys. Lipids 16 (1976) 285–291.

[5] F. Pattus, C. Rothen, M. Streit, P. Zahler, Further studies on the spreading of biomembranes at the air–water interface, Biochim. Biophys. Acta 647 (1981) 29–39.

[6] R.O. Calderón, B. Maggio, T.J. Neuberger, G.H. De Vries, Surface behavior of axolemma monolayers: physico-chemical characterization and use as supported planar membranes for cultured Schwann cells, J. Neurosci. Res. 34 (1993) 206–218.

[7] R.O. Calderón, B. Maggio, T.J. Neuberger, G.H. De Vries, Modulation of Schwann cell P0 glycoprotein and galactocerebroside by the surface organization of axolemma, J. Neurosci. Res. 40 (1995) 349–358.

[8] R.G. Oliveira, R.O. Calderón, B. Maggio, Surface behavior of myelin monolayers, Biochim. Biophys. Acta 1370 (1998) 127–137.

[9] S. Subramaniam, H.M. McConnell, Critical mixing in monolayer mixtures of phospholipids and cholesterol, J. Phys. Chem. 91 (1987) 1715–1718.

[10] J.P. Slotte, Lateral domain formation in mixed monolayers containing cholesterol and dipalmitoylphosphatidylcholine or *N*-palmitoylsphingomyelin, Biochim. Biophys. Acta 1235 (1995) 419–427.

[11] L.D. Worthman, K. Nag, P.J. Davis, K.M.W. Keough, Cholesterol in condensed and fluid phosphatidylcholine monolayers studied by epifluorescence microscopy, Biophys. J. 72 (1997) 2569–2580.

[12] S.L. Keller, W.H. Pitcher III, W.H. Huestis, H.M. McConnell, Red blood cell lipids form immiscible liquids, Phys. Rev. Lett. 81 (1998) 5019–5022.

[13] C.L. Dietrich, L.A. Bagatolli, Z.N. Volovyk, N.L. Thompson, M. Levi, K. Jakobson, E. Gratton, Lipid rafts reconstituted in model membranes, Biophys. J. 80 (2001) 1417–1428.

[14] R.G. Oliveira, B. Maggio, Epifluorescence microscopy of surface domain microheterogeneity in myelin monolayers at the air–water interface, Neurochem. Res. 25 (2000) 77–86.

[15] M.A. Moscarello, A.W. Newmann, D.D. Wood, Thermotropic phase transition in normal human myelin as observed in a sensitive microcalorimeter, Biochim. Biophys. Acta 728 (1983) 201–205.

[16] L.S. Chia, J.E. Thompson, M.A. Moscarello, Alteration of lipid-phase behavior in multiple sclerosis myelin revealed by wide-angle X-ray diffraction, Proc. Natl. Acad. Sci. USA 81 (1984) 1871–1874.

[17] G. Ayala, P. Carmona, M. de Cózar, J. Monreal, Vibrational spectra and structure of myelin membranes, Eur. Biophys. J. 14 (1987) 219–225.

[18] B. Maggio, The surface behavior of glycosphingolipids in biomembranes: a new frontier of molecular ecology, Prog. Biophys. Mol. Biol. 62 (1994) 55–117.

[19] D.C. Carrer, B. Maggio, Phase behavior and molecular interactions in mixtures of ceramide with dipalmitoylphosphatidylcholine, J. Lipid Res. 40 (1999) 1978–1989.

[20] M. Bloom, E. Evans, O.G. Mouritsen, Physical properties of the fluid lipid-bilayer component of cell membranes: a perspective, Q. Rev. Biophys. 24 (1991) 293–297.

[21] G.L. Gaines, in: I. Prigogine (Ed.), Insoluble Monolayers at Liquid-Gas Interfaces, Interscience Monographs on Physical Chemistry, John Wiley and Sons, New York, 1966.

[22] H. Möhwald, Phospholipid monolayers, in: R. Lipowsky, E. Sackman (Eds.), Handbook of Biological Physics, Vol. 1A, Structure and Dynamics of Membranes, Elsevier Science B.V., New York, 1995, pp. 161–211.

[23] D. Höning, D. Möbius, Direct visualization of monolayers at the air–water interface by Brewster angle microscopy, J. Phys. Chem. 95 (1991) 4590–4592.

[24] S. Henon, J. Meunier, Microscope at the Brewster angle: direct observation of first-order phase transitions in monolayers, Rev. Sci. Instrum. 62 (1991) 936–939.

[25] R. Peters, K. Beck, Translational diffusion in phospholipid monolayers measured by microphotolysis, Proc. Natl. Acad. Sci. USA 80 (1983) 7183–7187.

[26] H.M. McConnell, L.K. Tamm, R.M. Weis, Periodic structures in lipid monolayer phase transition, Proc. Natl. Acad. Sci. USA 81 (1984) 3249–3253.

[27] P.M. Elias, D.S. Friend, J. Goerke, Membrane sterol heterogeneity. Freeze-fracture detection with saponins and filipin, J. Histochem. Cytochem. 27 (1979) 1247–1260.

[28] S. Scott, S.A. Pendlebury, C. Green, Lipid organization in erythrocyte membrane microvesicles, Biochem. J. 224 (1984) 285–290.

[29] S. Mukhopadhyay, W. Cho, Interactions of annexin V with phospholipid monolayers, Biochim. Biophys. Acta 21 (1996) 58–62.

[30] J.E. Haley, F.G. Samuels, R.W. Ledeen, Studies of myelin purity in relation to axonal contamination, Cell. Mol. Neurobiol. 1 (1981) 175–178.

[31] C. Wüthrich, A.J. Steck, A permeability change of myelin membrane vesicles toward cations is induced by MgATP but not by phosphorylation of myelin basic protein, Biochim. Biophys. Acta 640 (1981) 195–206.

[32] F. Gonzales-Sastre, The protein composition of isolated myelin, J. Neurochem. 17 (1970) 1049–1056.

[33] J. Folch, M. Lees, G.H. Sloane-Stanley, A simple method for the isolation and purification of total lipids from animal tissues, J. Biol. Chem. 226 (1957) 497–509.

[34] G.R. Bartlett, Phosphorous assay in column chromatography, J. Biol. Chem. 234 (1959) 466–468.

[35] O.H. Lowry, N.J. Rosenbrough, A.L. Farr, R.J. Randall, Protein measurement with the Folin phenol reagent, J. Biol. Chem. 193 (1951) 265–275.
[36] D.A. Kirschner, A.L. Ganser, D.L.D. Caspar, Diffraction studies of molecular organization and membrane interactions in myelin, in: P. Morell (Ed.), Myelin, 2nd edn., Plenum Press, New York, 1984, pp. 51–95.
[37] H.M. McConnell, Equilibration rates in lipid monolayers, Proc. Natl. Acad. Sci. USA 93 (1996) 15001–15003.
[38] V. von Tscharner, H.M. McConnell, Physical properties of lipid monolayers on alkylated planar glass surface, Biophys. J. 36 (1981) 421–427.
[39] D. Höning, D. Möbius, Reflectometry at the Brewster angle and Brewster angle microscopy at the air–water interface, Thin Solid Films 210/211 (1992) 64–68.
[40] W. Frey, W.R. Schief Jr., V. Vogel, Two-dimensional crystallization of streptavidin studied by quantitative Brewster angle microscopy, Langmuir 12 (1996) 1312–1320.
[41] J.H. Ipsen, G. Karlstrom, O.G. Mouritsen, H. Wennerstrom, M.J. Zuckermann, Phase equilibria in the phosphatidylcholine-cholesterol system, Biochim. Biophys. Acta 905 (1987) 162–172.
[42] A. Radhakrishnan, H.M. McConnell, Condensed complexes of cholesterol and phospholipids, Biophys. J. 77 (1999) 1507–1517.
[43] H.M. McConnell, Structures and transitions in lipid monolayers at the air–water interface, Annu. Rev. Phys. Chem. 42 (1991) 171–195.
[44] D.J. Benvegnu, H.M. McConnell, Line tension between liquid domains in lipid monolayers, J. Phys. Chem. 96 (1992) 6820–6824.
[45] W.T. Norton, W. Cammer, Isolation and characterization of myelin, in: P. Morell (Ed.), Myelin, 2nd edn., Plenum Press, New York, 1984, pp. 147–195.
[46] M. Draper, M.B. Lees, D.S. Chan, Isoelectric focusing of proteolipid, J. Neurochem. 31 (1978) 1095–1099.
[47] H. Suda, Y. Tsukada, Improved method for purification of 2′,3′-cyclic nucleotide 3′-phosphohydrolase from bovine cerebral white matter, J. Neurochem. 34 (1980) 941–949.
[48] P.J. Brophy, Interactions of lipids with proteins of myelin and its associated cytoskeleton, in: R.E. Martenson (Ed.), Myelin: Biology and Chemistry, CRC Press, Boca Raton, FL, 1992, pp. 197–212.
[49] H. Möhwald, Phospholipid and phospholipid–protein monolayers at the air/water interface, Annu. Rev. Phys. Chem. 41 (1990) 441–476.
[50] D. Marsh, Lipid–protein interactions and heterogeneous lipid distribution in membranes, Mol. Membr. Biol. 12 (1995) 59–64.
[51] T. Gil, J.H. Ipsen, O.G. Mouritsen, M.A. Sabra, M.M. Sperotto, M.J. Zuckermann, Theoretical analysis of protein organization in lipid membranes, Biochim. Biophys. Acta 1376 (1998) 245–266.
[52] P.E. Braun, Molecular organization of myelin, in: P. Morell (Ed.), Myelin, 2nd edn., Plenum Press, New York, 1984, pp. 97–116.
[53] A.G. Lee, Myelin: delivery by raft, Curr. Biol. 11 (2001) R60–R62.
[54] M. Simons, E.M. Kramer, C. Thiele, W. Stoffel, J. Trotter, Assembly of myelin by association of proteolipid protein with cholesterol- and galactosylceramide-rich membrane domains, J. Cell Biol. 151 (2000) 143–153.